OncoTargets and Therapy

Dovepress
open access to scientific and medical research

Open Access Full Text Article

ORIGINAL RESEARCH

# RETRACTED ARTICLE: CXCL8 Promotes Glioma Progression By Activating The JAK/STAT1/HIF-1α/Snail Signaling Axis

This article was published in the following Dove Press journal:
*OncoTargets and Therapy*

Zhiming Chen[1,*]
Lei Mou[1,*]
Yiheng Pan[1]
Chi Feng[1]
Jingjing Zhang[2]
Junjun Li[3]

[1]Department of Neurosurgery, Taihe Hospital, Hubei University of Medicine, Shiyan 442000, Hubei, People's Republic of China; [2]Department of Obstetrics, Taihe Hospital, Hubei University of Medicine, Shiyan 442000, Hubei, People's Republic of China; [3]Department of Neurosurgery, Union Hospital, Tongji Medical College, Huazhong University of Science and Technology, Wuhan 430022, People's Republic of China

*These authors contributed equally to this work

**Background:** Upregulation of CXCL8 (C-X-C motif ligand 8) in tumor cells has been reported in several types of cancer, and it correlates with a poor prognosis. However, the role of CXCL8 in glioma progression remains unknown.
**Materials and methods:** In this study, we examined CXCL8 expression levels in human glioma cell lines and in sixteen human gliomas with different grades. The molecular role of CXCL8 in glioma cells was investigated using quantitative polymerase chain reaction (qRT-PCR) assays, Western blotting, CCK-8 assays, EdU assays, colony formation assays, Transwell migration and invasion assays.
**Results:** We found that high expression levels of CXCL8 were positively associated with progression and poor prognosis in human glioma. Mechanistically, CXCL8 promoted the epithelial-mesenchymal transition (EMT) of glioma cells by activating the JAK/STAT1/HIF-1α/Snail signaling pathway.
**Conclusion:** Taken together, our data provide a plausible mechanism for CXCL8-modulated glioma progression, which suggests that CXCL8 may represent a potential therapeutic target in the prevention and treatment of gliomas.
**Keywords:** glioma, progression, CXCL8, JAK/STAT1/HIF-1α/Snail



## Introduction

The glioma is the most prevalent tumor type in the central nervous system (CNS), and both its incidence and mortality rates have increased in recent years.[1–3] Progression of the tumor leads to a poor 5-year survival rate.[4] Although many studies on tumor progression have been carried out for many years, its complex mechanisms have not been fully elucidated. Thus, a better understanding of the unique molecular mechanisms underlying glioma tumor progression is an urgent task.

Tumor cell migration and invasion are the key steps during tumor progression.[5,6] EMT is a dynamic cellular process that is involved in tumor progression. During EMT, epithelial tumor cells lose basal-apical polarity and become motile mesenchymal cells, which have been implicated in tumor progression.[7] Of course, countless signaling pathways have been reported to be involved EMT regulation.[8,9]

CXCL8 (Interleukin-8 (IL-8)), one of the elastin-like recombinamer (ELR) motif-positive CXC-chemokine family members, is secreted by leukocytes, macrophages, endothelial cells, epithelial cells, airway smooth muscle cells and tumor cells.[10,11] It is initially produced as a 99 amino acid protein that undergoes cleavage to form an active CXCL8 isoform and a 72 amino acid peptide for monocytes and macrophages or a 77 amino acid peptide in nonimmune cells.[12,13] CXCL8 is encoded by a gene of the same name, which is located on chromosome 4q13-q21.

Correspondence: Junjun Li
Department of Neurosurgery, Union Hospital, Tongji Medical College, Huazhong University of Science and Technology, Jiefang Street, Wuhan 430022, People's Republic of China
Tel +86 15927413108
Fax +86 02785351619
Email ljj19891105@126.com




http://doi.org/10.2147/OTT.S224721

In this study, we determined that CXCL8 is correlated with tumor progression in glioma patients. Moreover, high levels of CXCL8 induce EMT via the JAK/STAT1/HIF-1α/Snail signaling pathway to promote tumor cell proliferation, migration and invasion. In addition, the expression levels of CXCL8 are a prognostic factor in glioma patients, suggesting that CXCL8 may be a potential therapeutic target for treating gliomas.

# Materials And Methods

## Bioinformatics Database

For the glioma expression microarray analysis, all data were obtained from ONCOMINE (www.oncomine.org/), Bredel Brain (IMAGE: 549933),[14] and Liang Brain (AA082747).[15]

## Cell Lines And Reagents

HA and NHA cells were cultured in astrocyte medium (Carlsbad, CA, USA), and the other cells (H4, A-172, U-251MG, LN-18, U-138MG and U-87MG (glioblastoma of unknown origin)) were cultured as described previously.[16,17] All cell lines were authenticated by short tandem repeat (STR) analysis and confirmed to be mycoplasma negative every 3 months. S3I-201 and WP1066 were purchased from SelleckChem (Selleck.cn, Houston, Texas, USA). The anti-CXCL8 antibody (ab7747) and the anti-HIF-1α antibody (ab92498) were purchased from Abcam (USA), anti-JAK (9945), anti-p-JAK (66245), anti-STAT1 (14995), anti-p-STAT1 (Ser727) (8826), anti-STAT2 (72604), anti-p-STAT2 (Tyr690) (88410), anti-STAT3 (4904), anti-p-STAT3 (Tyr705) (9145), and anti-β-actin (4970) antibodies were purchased from Cell Signaling Technology (Beverly, MA, USA).

## Patients And Sample Preparation

Seventy surgically resected glioma samples were collected between October 201[illegible] and May 2019 at Union Hospital. Four normal brain tissues were derived from patients with diffuse brain tissue swelling caused by severe car accidents who had to undergo partial nonfunctional area normal brain tissue resection. The purpose of this treatment was to decompress brain tissue. Ethical consent was approved by the ethics committee involving human subjects at Tongji Medical College, Huazhong University of Science and Technology (S360). Written informed consent was obtained from all patients before sample collection. All methods were performed in accordance with approved guidelines. Prior to glioma resection, no patient had received radiotherapy or chemotherapy. All samples were immediately snapfrozen in liquid nitrogen and stored in liquid nitrogen until they were used. This research was performed in accordance with the Declaration of Helsinki.

## Plasmid Construction And Transfection

To establish stable knockdown and overexpression cell lines, full-length shRNA sequences that specifically target CXCL8 or Snail were cloned into pLKO.1-MSCV-Puro or pcDNA3.0 vectors and were bidirectionally sequenced. Sequences of all shRNAs are provided in Supplementary Table 1. The construction of the plasmid and the packaging of the lentivirus were completed by GenePharma (Shanghai, China). Cells were infected by the lentivirus according to the manufacturer's protocol and were selected by treatment with puromycin (Sigma-Aldrich, St Louis, MO, USA) for two weeks to obtain cell lines with stable expression. The empty vector pcDNA3.0 or pLKO.1 and scrambled shRNA were used as negative controls.

## Cell Proliferation Assays

For the CCK-8 (Cell Counting Kit-8) assay, cells were counted and plated in complete culture medium at 3600 cells/well in 96-well plates. After treatment with 10 μL CCK-8 (Dojindo Laboratories, Japan), the absorbance at 450 nm was detected using a microplate reader (Spectra Max M2 reader, Molecular Devices, USA) and each experiment was performed in triplicate.

## EdU Proliferation Assay

Followin the indicated treatment, newly synthesized DNA in U-251MG and U-87MG cells was measured by EdU fluorescence staining based on the manufacturer's protocol (Click-iT® EdU Imaging Kits, Invitrogen). The cells, cultured in 96-well plates at a density of $8 \times 10^3$ cells/well, were labeled with 10 μM EdU, incubated for 3 h, and then fixed for 20 min with 3.7% formaldehyde at room temperature. Then, the fixative was removed, and the cells in each well were washed three times with 3% BSA in PBS. The BSA solution was removed, and the cells were permeabilized with 0.5% Triton X-100 (Sigma, San Francisco, CA, USA) for 20 min at room temperature. After washing the cells three times with 3% BSA in PBS, a 100 μL of Click-iT® reaction cocktail was added to each well, and the plate was incubated for 30 min at room temperature in the dark. Then, 1 mL of Hoechst 33342 nuclear staining solution (Sigma, San Francisco, CA, USA) was added to each well, and the plate was incubated for 25 min at room temperature in the dark. Subsequently, the staining solution was removed, and the cells were washed three times with PBS.

Then, the EdU-labeled cells were photographed and counted using a fluorescence microscope (CKX41-F32FL, Olympus, Tokyo, Japan). Image-Pro Plus software (Version 5.0, MD, USA) was used to determine the percentage of EdU-positive (EdU+) cells.

## Colony Formation Assay

A total of 3 mL of complete medium containing 500 cells per well was seeded in 6-well plates. The cells were cultured at 37°C and 5% $CO_2$ for two weeks, and the medium was not changed during this period. Then, the wells were washed with PBS three times, and the cells were fixed with 4% formaldehyde. The colonies were stained with 0.1% crystal violet (Servicebio, Wuhan, China). Finally, the colonies with a diameter > 2 mm were photographed and counted under an inverted microscope. All experiments were independently repeated three times.

## Cell Migration And Invasion Assays

Cell migration and invasion experiments were performed using the Transwell system (Corning, NY) based on the manufacturer's instructions. To assess invasion, filters were precoated with Matrigel (BD Biosciences, San Josè, CA, USA). Approximately $8 \times 10^4$ cells were added into the upper chamber containing serum-free DMEM. The bottom chamber contained 500 microliters of DMEM supplemented with 20% fetal bovine serum (FBS). Following 24 h of incubation, the cells on the upper surface were gently removed with a cotton swab, and then the membrane was fixed with 4% formaldehyde for 20 min and stained with 0.1% crystal violet solution (Servicebio, Wuhan, China) for 30 min. The cells that migrated to the lower surface of the membrane were photographed and counted under a microscope. The same experiment was performed for the migration assays, except that the filters were not precoated with Matrigel.

## Dual Luciferase Reporter Assay

U-251MG and U-87MG cells were routinely plated in 24-well plates for 24 h before transfection. The cells were transfected with a JAK/STAT firefly luciferase reporter plasmid and phRL-TK (Origene, Rockville, MD, USA) using Lipofectamine™ 3000 (Invitrogen, CA, USA) according to the manufacturer's protocol. The Renilla luciferase expression plasmid acted as an internal control. Then, the cells were harvested 24 h posttransfection and lysed with 100 µL of passive lysis buffer (Boster, Wuhan, China). Subsequently, the luciferase activities were determined with the Dual-Glo Luciferase Kit (Promega, USA).

## Cignal Finder Cancer 10-Pathway Reporter Array

Pathway analyses were performed with the Cignal Finder Cancer 10-Pathway Reporter Array (QIAGEN, Germany) according to the manufacturer's instructions. The suspended cells ($9 \times 10^3$/mL, 60 µL/well) were seeded into 96-well plates containing luciferase reporters for common targets in cancer pathways. Then, the cells were incubated at 37°C and 5% $CO_2$ for 24 h, and luciferase activity analyses were performed using the Dual-Luciferase Reporter Kit (Promega, USA).

## Western Blotting

All processes were performed as described previously.[16,17] The cells were lysed by electrophoresis on a 12% SDS-PAGE gel at 120 V for 2 h and were then transferred to a PVDF membrane (Millipore, Massachusetts, USA). The membrane was blocked with 5% fat-free milk in PBS for 2 h. Next, the membranes were incubated with primary and secondary antibodies and visualized using a chemiluminescent reagent (Thermo Fisher).

## RT-PCR

Total RNA was lysed from glioma samples using TRIzol reagent (Invitrogen). cDNA synthesis and real-time PCR were performed using the SYBR® Premix Ex Taq™ Kit (Takara, Japan). GAPDH acted as an internal control. The sequences of the CXCL8 primers were as follows: forward, 5′-ACTGAGAGTGATTGAGAGTGGAC-3′; reverse, 5′-AACCCTCTGCACCCAGTTTTC-3′. The sequences of the Snail primers were as follows: forward, 5′-TCGGAAGCCTA ACTACAGCGA-3′; reverse, 5′-AGATGAGCATTGGCAGC GAG-3′. Relative mRNA expression levels were normalized as described previously.[16,17]

## Immunofluorescence And Immunohistochemical Staining

Immunofluorescence (IF) staining was performed as described previously.[16,17] Cells were seeded in 24-well plates and fixed with 4% formaldehyde. After fixation, the cells were permeabilized with 0.5% Triton X-100 and blocked with 5% bovine serum albumin (BSA) in PBS for 1 h at room temperature. Then, the cells were incubated with the corresponding antibody in PBS containing 0.3% BSA and were finally incubated with a Cy3-conjugated secondary antibody (1:100, Promoter, China) in PBS containing 0.3% BSA. Fluorescence was visualized using laser scanning confocal microscope (Olympus, Japan).

Immunohistochemistry and semiquantitative scoring techniques were performed as described previously.[16,17] The percentage of positive staining was scored as follows: 0 (no positive signal), 1 (0–10% positive signal), 2 (10–30% positive signal), 3 (30–70% positive signal), and 4 (70–100% positive signal). The staining intensity was graded as follows: 1 (no staining), 2 (weak staining), 3 (moderate staining), and 4 (strong staining). The staining index (SI) was multiplied with possible scores of 0, 1, 2, 3, 4, 6, 8, 9, 12, and 16, and the median value was SI = 8, which was chosen as the cut off value. Therefore, samples with SI ≥ 8 were considered to have high expression, and samples with SI < 8 were considered to have low expression. IHC analyses were independently performed by two experienced pathologists who were blinded to the tissue information to avoid evaluation biases.

## Statistical Analyses

All data are presented as the mean ± standard deviation (SD) from at least 3 independent experiments. The unpaired/paired Student's *t* test was used to identify statistically significant data between two groups and one-way ANOVA followed by Dunnett's multiple comparisons tests was used to identify statistically significant data between more than two groups. Overall survival (OS) and disease-free survival (DFS) were evaluated using the Kaplan–Meier method, and multivariate survival analyses were performed using a Cox regression model. All statistical analyses were performed using GraphPad Prism version 7 (GraphPad Inc., La Jolla, CA, USA). P-values < 0.05 were considered to be statistically significant.



# Results

## High Levels Of CXCL8 Are Associated With A Poor Prognosis In Human Glioma

Data from seven normal brain tissues (NB) and 57 glioblastoma (GBM) tissues were obtained from Oncomine.[14,15] By analyzing these bioinformatics data, we determined that the CXCL8 expression levels in GBM were significantly higher than they were in normal brain tissues (Figure 1A and B). The CXCL8 expression levels in normal brain tissues and different grades of glioma were measured by qRT-PCR. We also found that the CXCL8 expression levels in glioma were significantly higher than those in normal brain tissues, and they were consistently upregulated in high-grade gliomas (III + IV) (Figure 1C and D). Sixteen glioma samples were assessed for their CXCL8 expression levels by Western blotting, including four grade I, four grade II, four grade III and four grade IV samples. Western blotting results indicated that CXCL8 expression levels were significantly higher in high-grade gliomas (Figure 1E). Then, immunohistochemical (IHC) analysis was adopted to measure the CXCL8 expression levels in NB and glioma. As shown in Figure 1F, the IHC staining intensity of CXCL8 was notably different between NB and different grades of glioma; further, quantification analyses further proved that CXCL8 protein expression levels in glioma were significantly higher than they were in NB, and they were consistently elevated in high-grade gliomas (Figure 1G). The correlation between CXCL8 and clinico-pathological features of 70 glioma samples was statistically analyzed. The results indicated that high levels of CXCL8 were significantly associated with the Karnofsky Performance Scale (KPS) score ($p = 0.0003$) and tumor recurrence ($p = 0.0002$, Table 1). These results were consistent with the KPS as an independent predictor for survival.[18] As shown in Table 2, using Univariate Cox regression analyses, high levels of CXCL8 were correlated with a notably increased risk of tumor recurrence in glioma patients ($p = 0.0002$) compared to the risk of recurrence in patients with low expression levels (Table 2). Multivariate Cox regression analyses showed that CXCL8 could predict poor prognosis when CXCL8 expression levels ($p = 0.035$), tumor grade ($p = 0.016$) and tumor recurrence ($p = 0.004$) were included in the analysis (Table 2). These results demonstrate a significant correlation between CXCL8 expression levels and prognosis. Furthermore, the Kaplan-Meier analysis indicated that high levels of CXCL8 were significantly associated with poorer disease-free survival (DFS) and overall survival (OS) rates in glioma patients (Figure 1H and I).

## High Levels Of CXCL8 Promote Glioma Cell Proliferation

First, we measured CXCL8 expression levels by qRT-PCR and Western blotting in two human brain gliocyte cell lines (HA and NHA) and six human brain glioma cell lines (U-251MG, U-138MG, H4, A-172, LN-18 and U-87MG). The results demonstrated that expression levels were high in the glioma cell line compared with the expression in the human brain gliocyte cell line (supplementary figures S1A). U-251MG and U-87MG cells were stably transfected with lentiviruses containing CXCL8, and their overexpression efficiency was verified by qRT-PCR and Western blotting (Figure 2A and B). Then, we employed CCK-8, EdU, and colony formation assays to clarify the effect of CXCL8 on

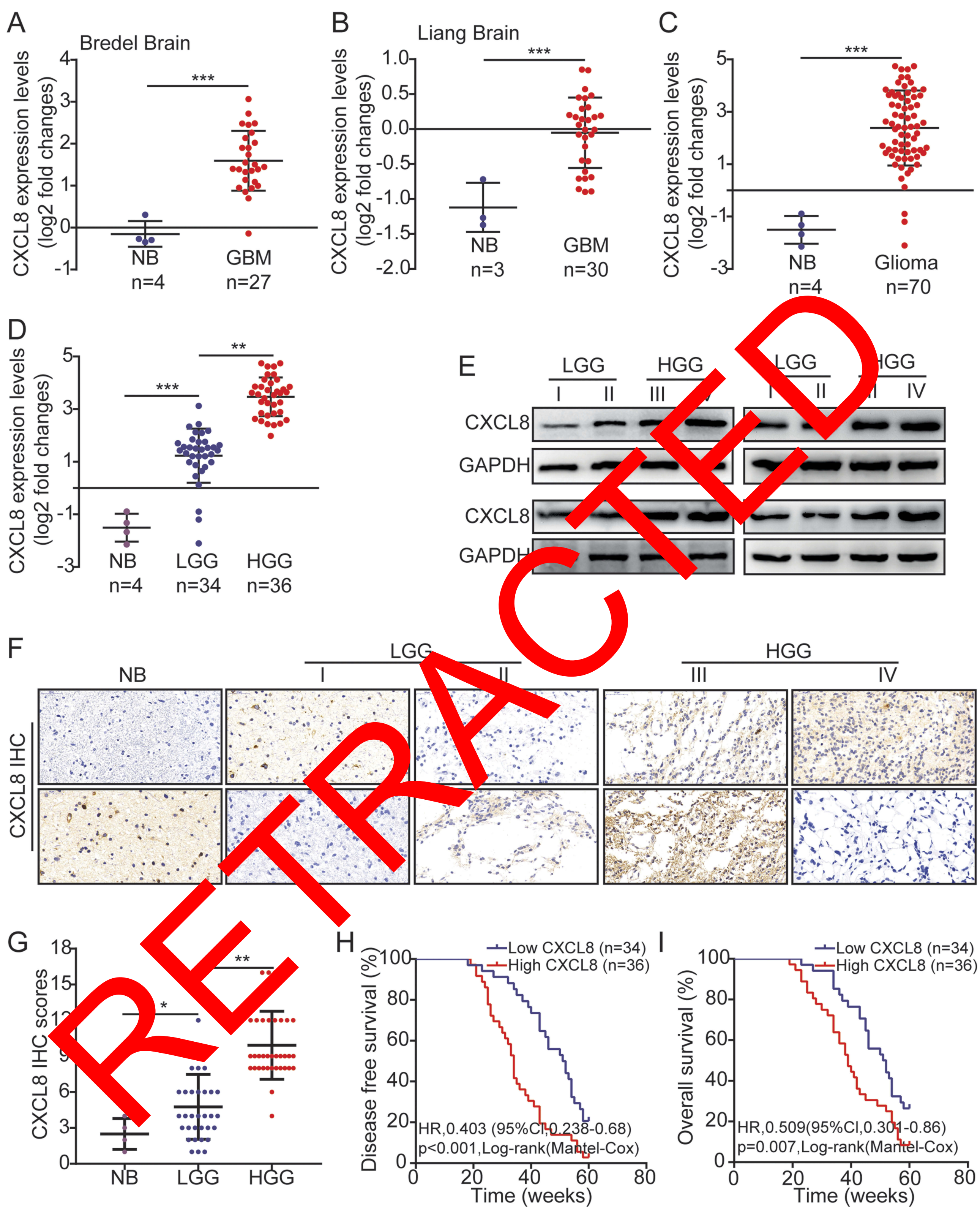


**Figure 1** High levels of CXCL8 are associated with poor prognosis in human glioma. (**A, B**) The expression levels of CXCL8 in NB and GBM obtained from the Oncomine database. The nonparametric Mann–Whitney U-test was used. (**C, D**) Relative CXCL8 expression levels measured by qRT-PCR in 4 NB, 34 LGG (Low-grade glioma) and 36 HGG (High-grade tissue). (**E**) Sixteen glioma tissues were measured for CXCL8 expression by Western blotting, including four grade I, four grade II, four grade III and four grade IV. (**F, G**) Representative images (**F**) and scores (**G**) of the IHC of CXCL8 expression in the paraffin-embedded different grade glioma. (**H, I**) Kaplan–Meier curves for DFS (**H**) and OS (**I**) of glioma patients with low vs high expression of CXCL8. The median CXCL8 expression levels were used as the cutoff value. Statistical significance was assessed using two-tailed Student's *t* test (**A, B, C, H** and **I**) and one-way ANOVA followed by Dunnett's tests for multiple comparisons (**D** and **G**). Scale bars: 50μm. *p < 0.05, **p < 0.01 and ***p < 0.001.

**Table 1** Association Of CXCL8 Expression With Clinicopathological Characteristics In Human Glioma

| Features | No. | CXCL8 | | P-value |
|---|---|---|---|---|
| | | Low | High | |
| Age, years | | | | |
| <50<br>≥50 | 40<br>30 | 18<br>16 | 22<br>14 | 0.49 |
| Gender | | | | |
| Male<br>Female | 37<br>33 | 20<br>14 | 17<br>19 | 0.33 |
| Tumor size, cm | | | | |
| <2<br>≥2 | 45<br>25 | 28<br>6 | 17<br>19 | 0.002 |
| Tumor location | | | | |
| Supratentorial<br>Subtentorial | 32<br>38 | 12<br>22 | 20<br>16 | 0.09 |
| Karnofsky performance scale | | | | |
| <90<br>≥90 | 36<br>34 | 10<br>24 | 26<br>10 | 0.0003 |
| WHO grade | | | | |
| Low-grade (I+II)<br>High-grade (III+IV) | 28<br>42 | 18<br>16 | 10<br>26 | 0.03 |
| Tumor recurrence | | | | |
| No<br>Yes | 22<br>48 | 18<br>16 | [illegible]<br>32 | 0.0002 |

tumor cell proliferation. These results showed that high levels of CXCL8 notably promoted tumor cell proliferation (Figure 2C–E). Then, we knocked down CXCL8 in U-251MG and U-87MG cells with short hairpin RNAs. The knockdown efficiency was also verified by qRT-PCR and Western blotting (supplementary Figure S2A and B). Subsequently, we adopted the above experiments to measure the effect of CXCL8 on tumor cell proliferation. These results indicated that CXCL8 knockdown obviously suppressed tumor cell proliferation (supplementary Figure S2C–E).

## High Levels Of CXCL8 Promote Glioma Cell Migration And Invasion

Subsequently, we employed Transwell migration and invasion assays to clarify the effect of CXCL8 on the migration and invasion of tumor cells. These results indicated that CXCL8 overexpression obviously promoted tumor cell migration and invasion (Figure 3A and B). However, CXCL8 knockdown notably suppressed tumor cell migration and invasion (Figure 3C and D).

## High Levels Of CXCL8 Promote Epithelial-Mesenchymal Transition In Glioma Cells

EMT is a reversible cell phenotype change that is closely related to normal development and tumor progression.[7] Characteristic E-cadherin downregulation is considered to be one of the key steps of EMT.[19] First, we observed cellular morphological changes to determine whether CXCL8 is involved in EMT. CXCL8 overexpression caused U-251MG cells to have a spindle-shaped morphology, which is consistent with a mesenchymal phenotype. However, CXCL8 knockdown caused U-87MG cells to have a typical epithelium-like phenotype (Figure 4A). Subsequently, we analyzed the expression level differences of EMT-related biomarkers between glioma cells with up- or downregulation of CXCL8. Immunofluorescence (IF) results indicated CXCL8 upregulation in U-251MG cells

**Table 2** Univariate And Multivariate Analyses Of Various Prognostic Parameters In Patients With Glioma Using Cox-Regression Analysis

| | Univariate Analysis | | | Multivariate Analysis | | |
|---|---|---|---|---|---|---|
| | p value | Hazard Ratio | 95% Confidence Interval | p value | Hazard Ratio | 95% Confidence Interval |
| CXCL8 | 0.02 | 1.187 | 1.112–2.362 | 0.035 | 1.121 | 1.115–2.164 |
| Tumor size, cm | 0.002 | 1.487 | 1.254–3.985 | 0.023 | 1.165 | 1.039–3.131 |
| Karnofsky performance scale | 0.0003 | 1.743 | 1.375–4.218 | 0.0041 | 1.398 | 1.256–3.972 |
| WHO grade | 0.03 | 1.135 | 1.103–2.265 | 0.016 | 1.231 | 1.185–2.869 |
| Tumor recurrence | 0.0002 | 1.892 | 1.691–4.389 | 0.004 | 1.342 | 1.218–3.527 |

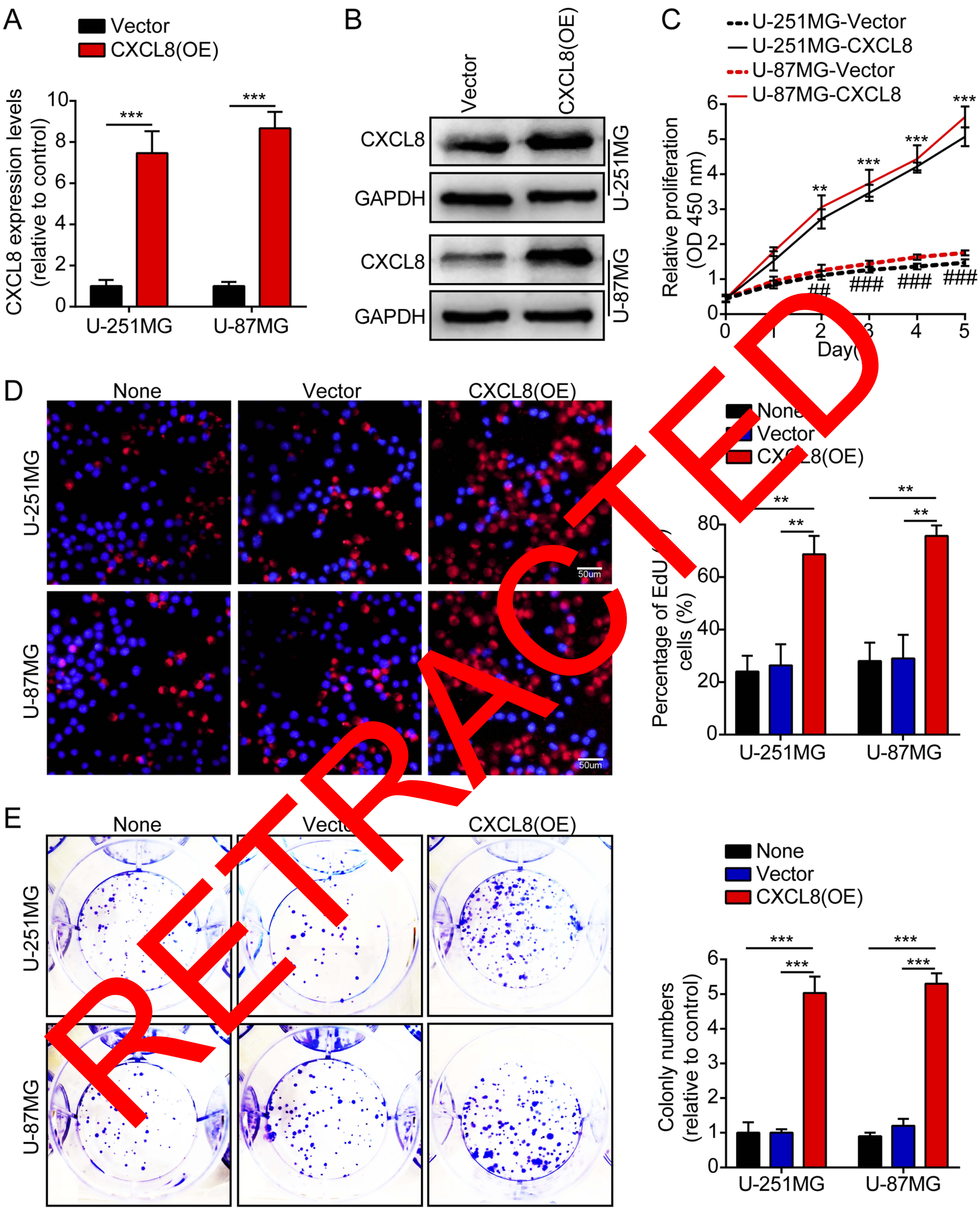




**Figure 2** High levels of CXCL8 promote glioma cells proliferation. (**A, B**) The over-expression efficiency against CXCL8 was verified by qRT-PCR and Western blotting in U-251MG and U-87MG cells. (**C**) Growth curves between Vector and CXCL8 (OE) by CCK-8 assay. The results are shown as the Mean ± Standard Deviation (SD) of three independent experiments. (**D, E**) Representative images (left panels) and histogram quantification (right panels) of the EdU (**D**) and colony formation assay (**E**) with U-251MG and U-87MG cells. Statistical significance was assessed using two-tailed Student's *t* test (**A, C**) and one-way ANOVA followed by Dunnett's tests for multiple comparisons (**D, E**). Scale bars: 50 μm. $^{**}p < 0.01$ and $^{***}p < 0.001$ or $^{\#\#}p < 0.01$ and $^{\#\#\#}p < 0.001$.

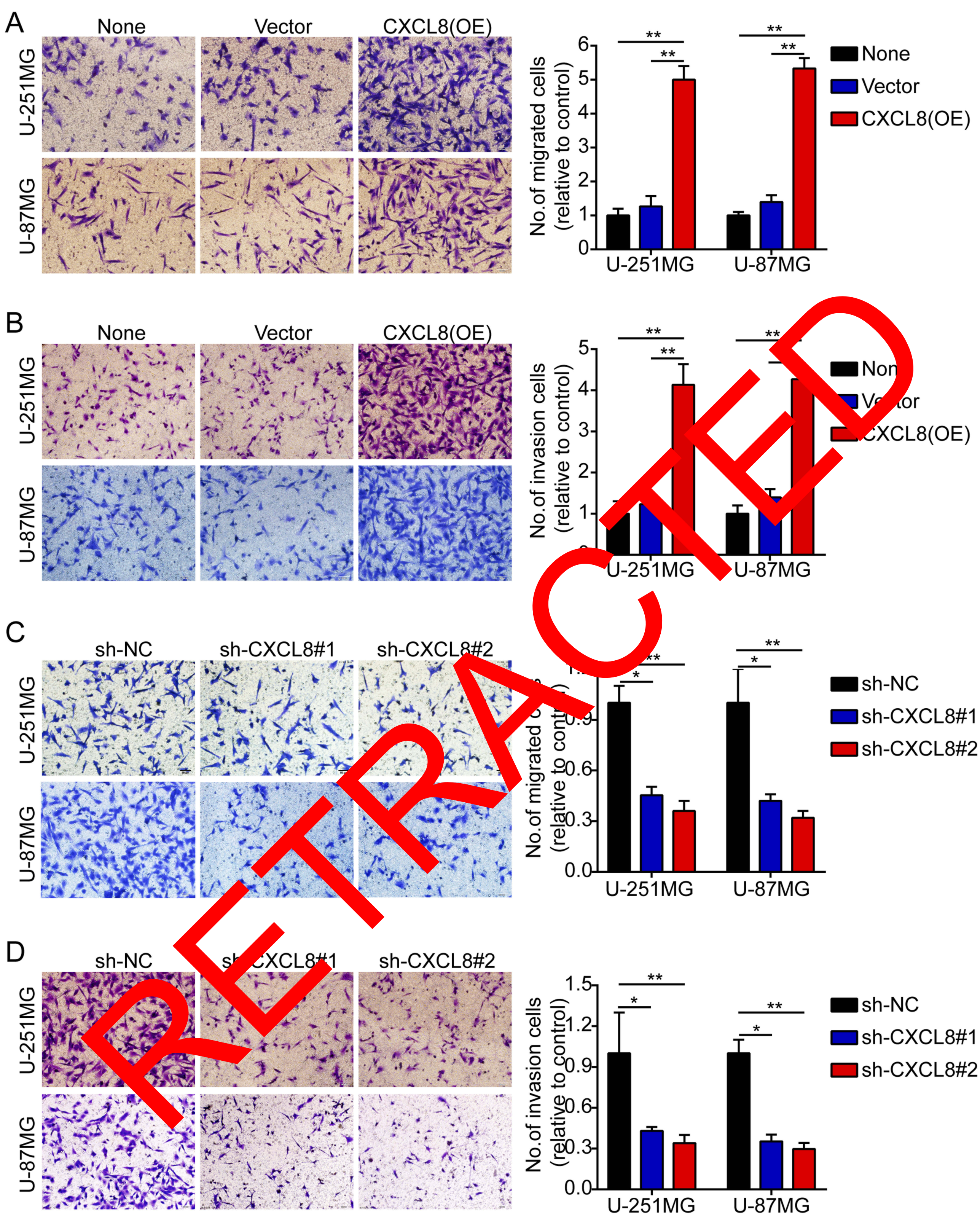


**Figure 3** High levels of CXCL8 promote glioma cells migration and invasion. (**A–D**). Representative images (left panels) and histogram quantification (right panels) of the Transwell migration (**A, C**) and invasion assays (**B, D**) with U-251MG and U-87MG cells. Statistical significance was assessed using one-way ANOVA followed by Dunnett's tests for multiple comparisons. Scale bars: 50 µm. *$p < 0.05$ and **$p < 0.01$.

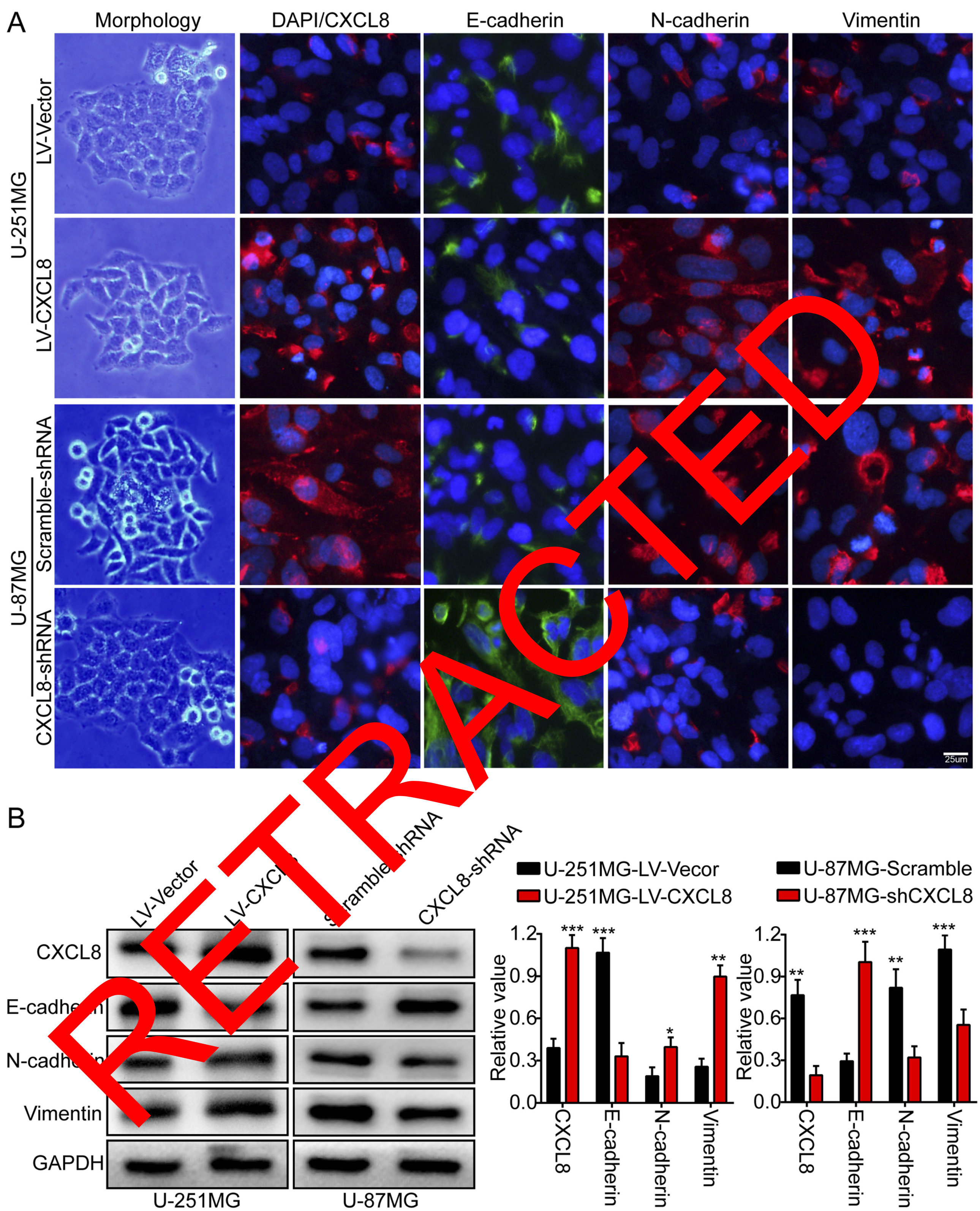


**Figure 4** High levels of CXCL8 promote glioma cells epithelial-mesenchymal transition. (**A**) Representative images of cellular morphology (left panel) and IF staining representing the expression levels of EMT-related biomarkers (right panel), E-cadherin, N-cadherin, and Vimentin, while over-expressing and knock downing CXCL8 expression in U-251MG and U-87MG cells. (**B**) Western blotting results demonstrating the protein expression levels of CXCL8, E-cadherin, N-cadherin and Vimentin in U-251MG and U-87MG cells with over-expressed and knockdown CXCL8. Representative images (left panels) and histogram quantification (right panels). Statistical significance was assessed using two-tailed Student's *t* test. Scale bars, 25µm. *p < 0.05, **p < 0.01 and ***p < 0.001.

decreased E-cadherin expression levels, while the mesenchymal biomarkers (N-cadherin and vimentin) were notably increased (Figure 4A). The opposite expression phenomena of these proteins were observed in CXCL8-knockdown U-87MG cells (Figure 4A). In addition, we further verified the EMT-related biomarker expression levels in both U-251MG and U-87MG cells by Western blotting (Figure 4B). These results demonstrate that CXCL8 contributes to glioma progression by promoting EMT.

## High Levels Of CXCL8 Promote EMT By The JAK/STAT1/HIF-1α/Snail Signaling Pathway In Glioma Cells

To clarify the potential mechanism of CXCL8-regulated glioma cell progression, Cignal Finder Cancer 10-Pathway Reporter Kits were adopted to screen for signaling pathways that might be involved in this process. The final results showed that the JAK/STAT signaling axis was obviously inhibited, but the other signaling axis was not notably affected by CXCL8 knockdown in U-251MG and U-87MG cells (supplementary figures S1B). To further verify this result, dual luciferase reporter assays were used in U-251MG and U-87MG cells. These results consistently showed that CXCL8 knockdown could markedly inhibit the JAK/STAT signaling axis, which was consistent with the signaling pathway screening outcome (supplementary figures S1B). Then, we knocked down CXCL8 with short hairpin RNAs in U-251MG and U-87MG cells and observed that the protein levels of p-JAK, p-STAT1, HIF-1α, and Snail obviously decreased compared with the levels in the control group. However, the other protein levels remained unchanged (Figure 5A). To verify these results, we cocultured CXCL8-overexpressing cells with two chemical inhibitors of the JAK/STAT signaling pathway, WP1066 and S3I-201. Initially, their inhibition efficiency in U-251MG and U-87MG cells was validated by p-JAK analysis (Figure 5B and B1). The p-STAT1 protein expression levels after CXCL8overexpression in U-251MG and U-87MG cells were attenuated by WP1066 and S3I-201 treatments (Figure 5B and B2). In addition, the HIF-1α and Snail protein expression levels after CXCL8overexpression in U-251MG and U-87MG cells were also attenuated by WP1066 and S3I-201 treatments (Figure 5B, B3 and B4). These data strongly indicate that CXCL8overexpression promoted Snail protein expression via the JAK/STAT1/HIF-1α signaling axis.

## Snail Is Involved In CXCL8-Regulated Glioma Cell Proliferation, Migration And Invasion

Accumulating evidence indicates that the HIF-1α/Snail signaling axis plays a vital role in regulating EMT.[20] Therefore, we speculated that CXCL8 might upregulate Snail expression, thereby promoting tumor cell proliferation, migration and invasion. First, to determine the correlation between CXCL8 and Snail, we measured the expression of CXCL8 and Snail in 70 glioma samples using qRT-PCR. The results showed that their expression is positively correlated (Figure 6A). Next, we overexpressed Snail in U-251MG and U-87MG cells to determine whether it is involved in CXCL8-regulated glioma cell progression (Figure 6B and C). As expected, Snail overexpression abrogated the effects of CXCL8 knockdown on inhibiting U-251MG and U-87MG cell proliferation (Figure 6D and E and supplementary figures S3A), colony formation (Figure 6F and supplementary figures S3B), migration (Figure 6G and supplementary figures S3C) and invasion (Figure 6H and supplementary figures S3D). In addition, our data also indicated that Snail overexpression obviously promoted U-251MG and U-87MG cell proliferation (supplementary figures S4A and B and supplementary figures S5A), colony formation (supplementary figures S4C and supplementary figures S5B), migration (supplementary figures S4D) and invasion (supplementary figures S4E). Taken together, our data prove that CXCL8 promotes the proliferation, migration and invasion of glioma cells by regulating Snail protein expression.

## Discussion

Although gliomas have been studied for many years, the underlying molecular mechanisms and the effective treatment of glioma remain unknown. Herein, we proved that CXCL8 is associated with tumor progression and correlated with a poor clinical outcome. In addition, we found that high levels of CXCL8 promoted glioma cell proliferation, migration and invasion by inducing EMT. Mechanistically, CXCL8 induced EMT via the JAK/STAT1/HIF-1α/Snail signaling axis.

The JAK/STAT signaling pathway plays an important role in tumor progression.[21,22] In this study, we used a dual luciferase reporter assay to screen possible signaling pathways and found that CXCL8 affects the JAK/STAT signaling axis. Accumulating evidence has indicated that STAT1 is also involved in the regulation of HIF-1α.[23,24] In addition,

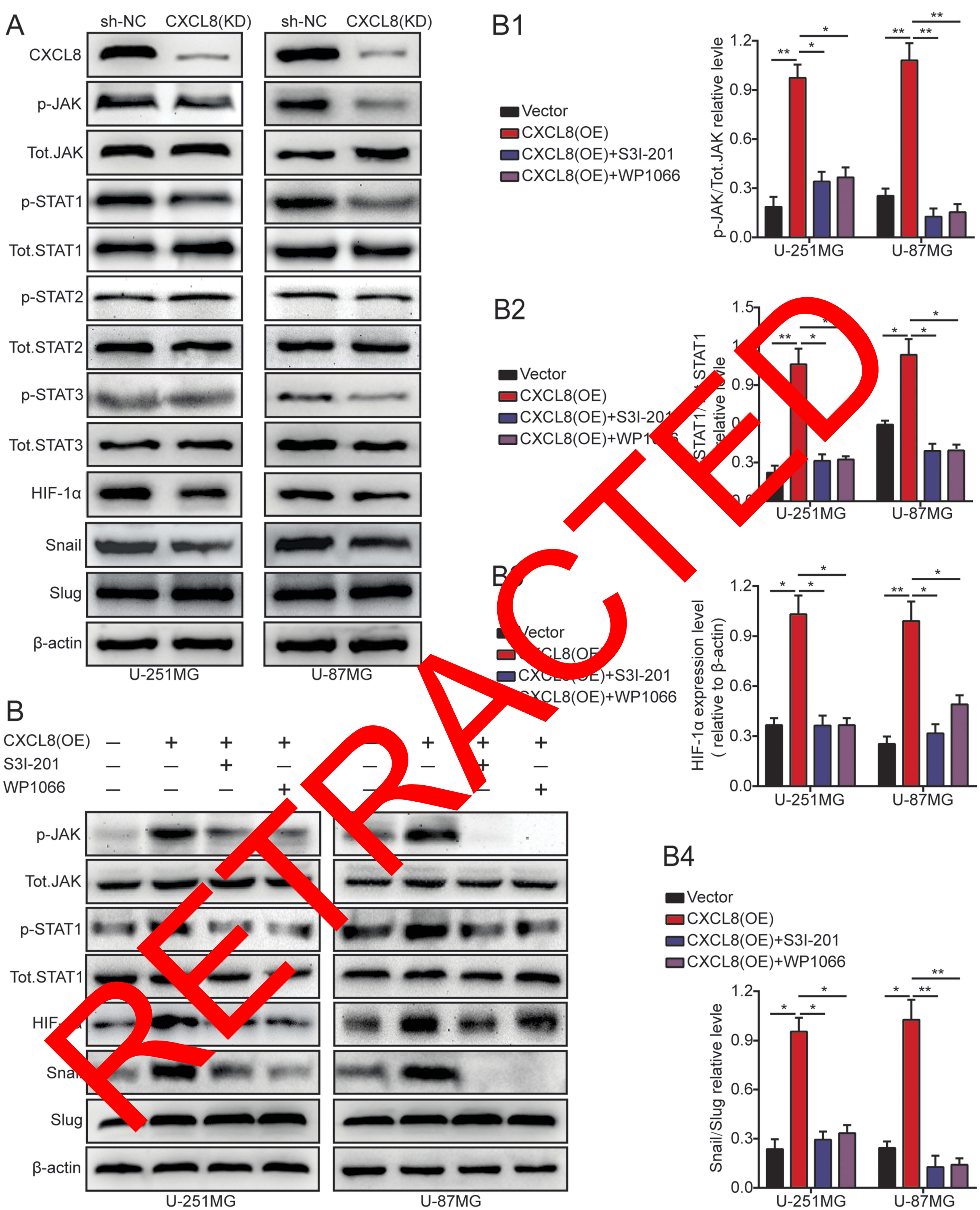


**Figure 5** High levels of CXCL8 promote the EMT by the JAK/STAT1/HIF-1α/Snail signal pathway in glioma cells.(**A**) CXCL8 knockdown decreased the protein level of p-JAK, p-STAT1, HIF-1α and Snail. Other proteins remain unchanged. (**B**) U-251MG and U-87MG cells transfected with CXCL8 plasmid and co-cultured with JAK/STAT signaling inhibitors were reaped, and the lysates were immuneblotted for p-JAK, Tot.JAK, p-STAT1, Tot.STAT1, HIF-1α, Snail and Slug. The histogram quantification (right panels) of p-JAK/Tot.JAK (**B1**), p-STAT1/Tot.STAT1 (**B2**), HIF-1α/β-actin (**B3**) and Snail/Slug (**B4**). Statistical significance was assessed using one-way ANOVA followed by Dunnett's tests for multiple comparisons. *p < 0.05 and **p < 0.01.

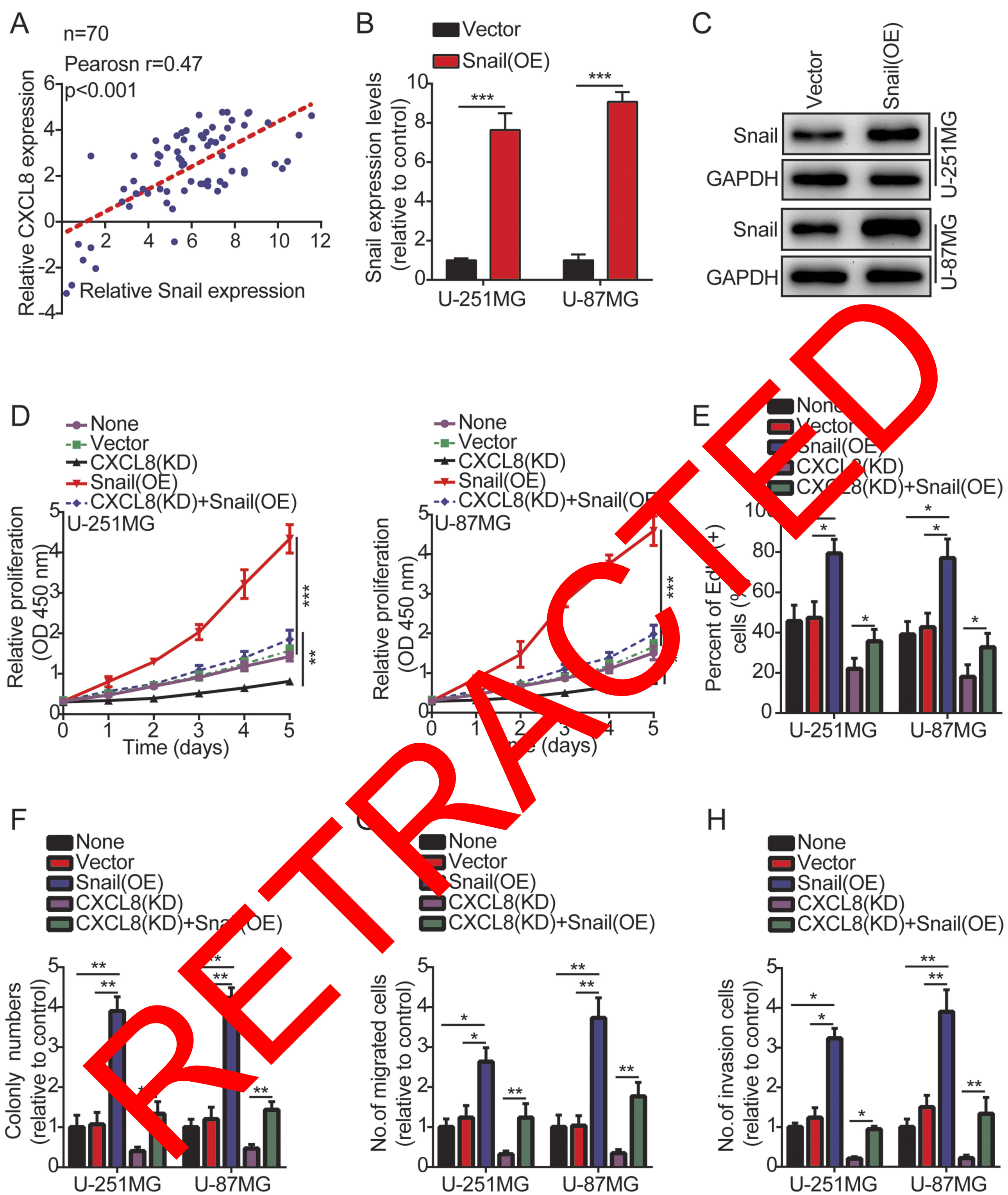




**Figure 6** Snail is involved in CXCL8-regulated glioma cells proliferation, migration and invasion. (**A**) Correlation analysis of CXCL8 and Snail mRNA expression by qRT-PCR. (**B, C**) The over-expression efficiency against Snail was verified by qRT-PCR and Western blotting in U-251MG and U-87MG cells. (**D**) Growth curves between None, Vector, CXCL8 (KD), Snail (OE) and CXCL8 (KD) + Snail (OE) by CCK-8 assay. The results are shown as the Mean ± Standard Deviation (SD) of three independent experiments. (**E–H**) The histogram quantification of the EdU (**E**), colony formation assay (**F**), Transwell migration (**G**) and invasion assays (**H**) with U-251MG and U-87MG cells. All the results indicated that Snail over-expression abrogated the effects of CXCL8 knockdown on inhibiting U-251MG and U-87MG cell proliferation (**D, E**), colony formation (**F**), migration (**G**) and invasion (**H**). Statistical significance was assessed using two-tailed Student's *t* test (**A** and **B**) and one-way ANOVA followed by Dunnett's tests for multiple comparisons (**D-H**). *$p < 0.05$, **$p < 0.01$ and ***$p < 0.001$.

numerous studies have indicated that the HIF-1α/Snail signaling pathway plays a vital role in regulating EMT.[20] Tissue hypoxia induces EMT, particularly for tumor cells, which enhances their migration and invasion.[25] In this study, our results indicated that CXCL8 knockdown decreased HIF-1α protein expression levels, leading to a reduction of the effect of Snail on the inhibition of E-cadherin. Interestingly, a previous study reported that hypoxia induces a Snail-activated EMT in tumor cells,[26,27] which is further support for our results. In addition, our results also indicated that knockdown of CXCL8 did not affect changes in Slug protein, suggesting that Slug was not a downstream effector of CXCL8 promoting glioma progression. Of course, there are many reports that Slug is involved in promoting the progression of glioma. Li et al reported that Nuciferine suppressed the GBM progression via targeting inhibition SOX2-AKT/STAT3-Slug axis.[28] Oh et al also reported that Slug exerted a vital role in promoting glioma invasion and chemotherapy resistance.[29] Lin et al also reported that STAT3/Slug signaling axis enhanced invasiveness and tumor stem cell characteristics of tumor cells induced by radiotherapy.[30] Accumulating evidence has proven that the functional loss of E-cadherin is the key step of EMT and that numerous transcription factors can suppress E-cadherin expression.[7,19] It has been reported that Snail can bind to the E-cadherin promoter and directly inhibit its transcription.[31,32] Herein, we observed that cells with high CXCL8 expression had greater expression of Snail. These data indicate that CXCL8 activates Snail to induce EMT.

Previously, our team also reported prognostic glioma markers.[16,17] Herein, we found that high levels of CXCL8 were associated with tumor progression in glioma patients. Importantly, patients with high levels of CXCL8 displayed poorer DFS and OS, showing that CXCL8 is a novel prognostic marker for glioma patients. In this study, high levels of CXCL8 contribute to tumor progression. Of course, there may be many other molecules involved in this process, which requires more research to determine.

## Conclusion

In summary, this study clarified the function and expression pattern of CXCL8 in glioma and found that high levels of CXCL8 are correlated with tumor progression and are a poor prognostic indicator for glioma patients. The high levels of CXCL8 induce EMT and enhance tumor cell proliferation, migration and invasion via activation of the HIF-1α/Snail signal axis. However, the role of CXCL8 in glioma progression has not been fully elucidated, and our research only reveals some of its molecular mechanisms for promoting EMT. Therefore, more research is needed to further elucidate the function of CXCL8 in tumors. Clarification of the JAK/STAT1/HIF-1α/Snail signaling axis may not only expand our knowledge of CXCL8-induced tumor progression but also develop a promising molecular therapeutic new strategy against this disease.

## Acknowledgments

The research was supported by the National Natural Science Foundation of China (No. 81571210; No. 30801180).

## Disclosure

The authors report no conflicts of interest in this work.

## References

1. Jia G, Wang Q, Wang R, et al. Tubeimoside-1 induces glioma apoptosis through regulation of Bax/Bcl-2 and the ROS/Cytochrome C/Caspase-3 pathway. *Onco Targets Ther*. 2015;8:303–309. doi:10.2147/OTT.S76063
2. [illegible], Li XT, Wu C, et al. miR-132 can inhibit glioma cells invasion and migration by target MMP16 in vitro. *Onco Targets Ther*. 2015;8:3211–3218. doi:10.2147/OTT.S79282
3. Thon N, Kreth S, Kreth FW. Personalized treatment strategies in glioblastoma: MGMT promoter methylation status. *Onco Targets Ther*. 2013;6:1363–1372. doi:10.2147/OTT.S50208
4. Jiang PF, Wang P, Sun XL, et al. Knockdown of long noncoding RNA H19 sensitizes human glioma cells to temozolomide therapy. *Onco Targets Ther*. 2016;9:3501–3509. doi:10.2147/OTT.S96278
5. Taube JH, Herschkowitz JI, Komurov K, et al. Core epithelial-to-mesenchymal transition interactome gene-expression signature is associated with claudin-low and metaplastic breast cancer subtypes. *Proc Natl Acad Sci U S A*. 2010;107(35):15449–15454. doi:10.1073/pnas.1004900107
6. Tan HX, Cao ZB, He TT, Huang T, Xiang CL, Liu Y. TGF beta 1 is essential for MSCs-CAFs differentiation and promotes HCT116 cells migration and invasion via JAK/STAT3 signaling. *Onco Targets Ther*. 2019;12:5323–5334. doi:10.2147/OTT.S178618
7. Thiery JP, Acloque H, Huang RYJ, Nieto MA. Epithelial-mesenchymal transitions in development and disease. *Cell*. 2009;139(5):871–890. doi:10.1016/j.cell.2009.11.007
8. Zhu LH, Chen W, Li GQ, et al. Upregulated RACK1 attenuates gastric cancer cell growth and epithelial-mesenchymal transition via suppressing Wnt/beta-catenin signaling. *Onco Targets Ther*. 2019;12:4795–4805. doi:10.2147/OTT.S205869
9. Yin JH, Wang L, Wang Y, Shen HL, Wang XJ, Wu L. Curcumin reverses oxaliplatin resistance in human colorectal cancer via regulation of TGF-beta/Smad2/3 signaling pathway. *Onco Targets Ther*. 2019;12:3893–3903. doi:10.2147/OTT.S199601
10. Matsushima K, Baldwin ET, Mukaida N. Interleukin-8 and MCAF: novel leukocyte recruitment and activating cytokines. *Chem Immunol*. 1992;51:236–265.
11. Hoffmann E, Dittrich-Breiholz O, Holtmann H, Kracht M. Multiple control of interleukin-8 gene expression. *J Leukoc Biol*. 2002;72(5):847–855.

12. Modi WS, Dean M, Seuanez HN, Mukaida N, Matsushima K, O'Brien SJ. Monocyte-derived neutrophil chemotactic factor (MDNCF/IL-8) resides in a gene cluster along with several other members of the platelet factor 4 gene superfamily. *Hum Genet*. 1990;84(2):185–187. doi:10.1007/bf00208938
13. Skelton NJ, Quan C, Reilly D, Lowman H. Structure of a CXC chemokine-receptor fragment in complex with interleukin-8. *Structure*. 1999;7(2):157–168. doi:10.1016/S0969-2126(99)80022-7
14. Bredel M, Bredel C, Juric D, et al. Functional network analysis reveals extended gliomagenesis pathway maps and three novel MYC-interacting genes in human gliomas. *Cancer Res*. 2005;65(19):8679–8689. doi:10.1158/0008-5472.CAN-05-1204
15. Liang Y, Diehn M, Watson N, et al. Gene expression profiling reveals molecularly and clinically distinct subtypes of glioblastoma multiforme. *Proc Natl Acad Sci U S A*. 2005;102(16):5814–5819. doi:10.1073/pnas.0402870102
16. Li JJ, Xu H, Wang QP, et al. Pard3 suppresses glioma invasion by regulating RhoA through atypical protein kinase C/NF-kappa B signaling. *Cancer Med*. 2019;8(5):2288–2302. doi:10.1002/cam4.2063
17. Li JJ, Xu H, Wang QP, Wang SH, Xiong NX. 14-3-3 zeta promotes gliomas cells invasion by regulating Snail through the PI3K/AKT signaling. *Cancer Med*. 2019;8(2):783–794. doi:10.1002/cam4.1950
18. Lacroix M, Abi-Said D, Fourney DR, et al. A multivariate analysis of 416 patients with glioblastoma multiforme: prognosis, extent of resection, and survival. *J Neurosurg*. 2001;95(2):190–198. doi:10.3171/jns.2001.95.2.0190
19. Kalluri R, Weinberg RA. The basics of epithelial-mesenchymal transition. *J Clin Invest*. 2009;119(6):1420–1428. doi:10.1172/JCI39104
20. Zhang J, Deng YT, Liu J, et al. Norepinephrine induced epithelial-mesenchymal transition in HT-29 and A549 cells in vitro. *J Cancer Res Clin Oncol*. 2016;142(2):423–435. doi:10.1007/s00432-015-2044-9
21. Xue W, Li W, Zhang T, et al. Anti-PD1 up-regulates PD-L1 expression and inhibits T-cell lymphoma progression: possible involvement of an IFN-gamma-associated JAK-STAT pathway. *Onco Targets Ther*. 2019;12:2079–2088. doi:10.2147/OTT.S187280
22. Sun Y, Liu L, Wang Y, et al. Curcumin inhibits the proliferation and invasion of MG-63 cells through inactivation of the p-JAK2/p-STAT3 pathway. *Onco Targets Ther*. 2019;12:2011–2021. doi:10.2147/OTT.S172909
23. Hiroi M, Mori K, Sakaeda Y, Shimada J, Ohmori Y. STAT1 represses hypoxia-inducible factor-1-mediated transcription. *Biochem Biophys Res Commun*. 2009;387(4):806–810. doi:10.1016/j.bbrc.2009.07.138
24. Parra-Izquierdo I, Castanos-Mollor I, Lopez J, et al. Lipopolysaccharide and interferon-gamma team up to activate HIF-1alpha via STAT1 in normoxia and exhibit sex differences in human aortic valve interstitial cells. *Biochim Biophys Acta Mol Basis Dis*. 2019;1865:2168–2179. doi:10.1016/j.bbadis.2019.04.014
25. Zavadil J, Haley J, Kalluri R, Muthuswamy SK, Thompson E. Epithelial-mesenchymal transition. *Cancer Res*. 2008;68(23):9574–9577. doi:10.1158/0008-5472.CAN-08-2316
26. Yang Z, Yu W, Huang R, Ye M, Min Z. SIRT6/HIF-1alpha axis promotes papillary thyroid cancer progression by inducing epithelial-mesenchymal transition. *Cancer Cell Int*. 2019;19:17. doi:10.1186/s12935-019-0730-4
27. Liu KH, Tsai YT, Chin SY, Lee WR, C[illegible]en YC, S[illegible] SC. Hypoxia stimulates the epithelial-to-mesench[illegible]al transition i[illegible] lung cancer cells through accumulation of nuclear [illegible]a-catenin. *An[illegible]cancer Res*. 2018;38(11):6299–6308. doi:1[illegible]21873/anti[illegible]res.1298[illegible]
28. Li Z, Chen Y, An T, et [illegible] Nuciferine inhi[illegible] t[illegible] progression of glioblastoma by suppre[illegible]ng the S[illegible]2-AKT/S[illegible]T3-Slug signaling pathway. *J Exp Clin Cance[illegible] Res*. [illegible]19;38(1):1[illegible]9. doi:10.1186/s13046-019-1134-y
29. Oh SJ, Ahn EJ, [illegible]n O, et al. The [illegible]le [illegible]yed by SLUG, an epithelial-mesenchym[illegible] trans[illegible]n factor, in i[illegible]sion and therapeutic resistance of malignant glioma. *Cell Mol Neurobiol*. 2019;39(6):769–782. doi:[illegible]/s10571-019-[illegible]77-5
30. L[illegible] JC, Tsai JT, Chao TY, Ma HI, Liu WH. The STAT3/slug axis [illegible]hances radiati[illegible]-induced tumor invasion and cancer stem-like p[illegible]perties in ra[illegible]oresistant glioblastoma. *Cancers*. 2018;10(12). do[illegible]0.3390/canc[illegible]s10110400
31. Lee [illegible] Nels[illegible] CM. New insights into the regulation of epithelial-mesenchymal transition and tissue fibrosis. *Int Rev Cell Mol Biol*. [illegible]94:171–221. doi:10.1016/B978-0-12-394305-7.00004-5
[illegible]. Perez-Moreno MA, Locascio A, Rodrigo I, et al. A new role for E12/E47 in the repression of E-cadherin expression and epithelial-mesenchymal transitions. *J Biol Chem*. 2001;276(29):27424–27431. doi:10.1074/jbc.M100827200


RETRACTED